Stress Analysis of Piping Elbows using FEM

Amran Ayob

Faculty of Mechanical Engineering, University of Technology Malaysia, 81310 UTM Skudai, Johor

(Received on 13 - 1 - 2003)

ABSTRACT

This study concerns the stress analysis of 90ß smooth piping elbows with circular cross section and straight tangent pipes. The finite element method (FEM) is used for stress analysis of elbows having a wide range of bend and pipe factors. The main aim of the study is to review the stress behaviour when an elbow is subjected to loadings of in-plane bending, torsion and internal pressure. The study includes the effect of end constraint, pipe factor, bend radius and load coupling behaviour. The study shows that the stress level is influenced by end constraint, pipe factor and bend radius, with thinner elbows being affected to a larger extent.

KEYWORDS

Elbows, pipe factor, pipe bend, tangent pipe, stress analysis, finite element method, stress indices, load interaction, combined loading.

NOMENCLATURE

r	pipe radius
d	pipe diameter
R	bend radius
t	thickness
b	bend factor = R/r_m
λ	pipe factor = tR/r_m^2
ϕ	axial (meridional) location, ϕ=0° at elbow mid-section
θ	hoop (circumferential) location, θ=0° at extrados
T	torsion
$\bar{T}$	non-dimensionalised first yield torsion
P	internal pressure
$\bar{P}$	non-dimensionalised first yield pressure
M	in-plane moment
$\bar{M}$	non-dimensionalised first yield in-plane moment
σ	stress

suffices

θ	hoop (circumferential) direction
ϕ	axial (meridional) direction
max	maximum
vM	von Mises
n	nominal
i	inner
o	outer
m	mean

INTRODUCTION

Elbows are used in piping systems for layout requirements and to give additional flexibility. During operation, various loads which are induced by thermal expansion or mechanical effects are transmitted to the curved region causing high stress levels. Flexibility and stresses in elbows have been extensively studied and have resulted in various formulae, some of which form the basis of the present piping design codes.

The first theoretical treatment of elbows was carried out by von Karman [1] who developed formulae for in-plane moment on simple elbows. Based on a similar energy method, Vigness [2] studied out-of-plane bending and Kafka and Dunn [3] studied the influence of internal pressure on in-plane bending. Rodabaugh and George [4] made a serious attempt to analyse the effect of internal pressure on stresses when the elbow is being subjected to in-plane or out-of-plane moments, and after some modification for hoop membrane stresses by Gross [5], the combined analyses formed the basis of the stress indices currently used in the nuclear piping code of ASME Section III [6]. The BS 806 [7] code is based on studies carried out by Turner and Ford [8] and Smith [9]. They accounted for mid-wall strain and did not limit the value of R/r_m, i.e. two of the limitations of the work by Rodabaugh [4].

Torsion and moment loading cause considerable cross-sectional ovalization in thin-walled elbows. The deformation is less at the bend ends where it is restricted by the stiffening effect of the attached pipes. Pardue and Vigness [10] carried out experiments on the end effects of elbows and noted that the presence of end constraints increases stiffness and reduces stresses. Findlay and Spence [11] presented an experimental and theoretical comparison for in-plane bending of elbows with flanged ends and noted that stresses increase with tighter bends and thinner elbows. In later years Lang [12] provided a complete description of the stress fields. Lang's model considers elbow ovalization which is useful in determining the discontinuity stress fields at the junction with the tangent pipe.

There have been many attempts to improve the stress indices used in design codes. Fujimoto and Soh [13] carried out finite element and experimental stress analyses on elbows which are beyond the application limit of most standard design procedures. Dodge and Moore [14] proposed stress indices for moment loadings based on the analysis of George and Rodabaugh [4]. So did other researchers such as Ohtsubo and Watanabe [15], Thomson and Spence [16] and Natarajan and Blomfield [17].

For a combination of loads applied simultaneously, the ASME [6] and BS [7] formulation is largely based on the maximum stress intensity (where ever it occurs) being equal to, or less than, the sum of the maximum stress intensities due to the loads taken individually. This gives a conservative design if the maximum stresses from the combining loads do not occur at the same location. In this study the maximum stress is obtained after the stresses from the individual loads are summed at their respective locations.

THE FINITE ELEMENT MODELS

This study looks at the main parameters which influence the performance of piping elbows, namely pipe dimensions and the applied load combinations. The analysis assumes linear elastic material behaviour and neglects initial geometrical imperfections. The pipe factor λ is chosen to be between 0.0267 and 1.4 and the bend factor b=2, 3, 5 and 7 so that the results can be compared to the BS and ASME codes. These values represent the range of piping elbows commonly used in power plants. The geometrical features of all 16 models, representing a wide range of b and λ, are given in Table 1. The models have a bend angle of 90° and a mean diameter, d_m= 0.2 m.

Table 1: Geometric dimensions of elbow models

Model	b	λ	d_m/t	Model	b	λ	d_m/t
EL01	2	0.0267	150	EL09	5	0.0667	150
EL02	2	0.05	80	EL10	5	0.125	80
EL03	2	0.2	20	EL11	5	0.5	20
EL04	2	0.4	10	EL12	5	1.0	10
EL05	3	0.04	150	EL13	7	0.0933	150
EL06	3	0.075	80	EL14	7	0.175	80
EL07	3	0.3	20	EL15	7	0.7	20
EL08	3	0.6	10	EL16	7	1.4	10

The same FE mesh was used throughout so that the node numbering is retained in all models. This simplifies the task of extracting stress data and performing load interaction analysis. The curved section was composed of 24 and 12 uniform elements in the hoop and axial directions respectively. The length of the attached tangent pipes was 4 times the mean diameter, and was considered to be adequate to prevent propagation of end boundary effects into the curved section. A total of 768, 20-node hexahedral elements and 5496 nodes were generated, using PATRAN [19] software. The linear static stress analysis was performed using the ASAS [20] finite element code

The first part of the analysis is aimed at confirming the elastic behaviour of the elbows when they are subjected to individual loads. The results are compared to those from theoretical analysis and design rules. The subsequent part deals with the first yield behaviour of elbows when two loads act simultaneously, assuming linear behaviour and the absence of load coupling effect. The results of the latter study provide the means of assessing the level of conservatism in present design rules.

This was followed by a geometrically nonlinear analysis which was carried out on two elbow models, EL01 and EL07. Model EL01 represents a thin elbow with a small bend radius and elbow model EL07 represents a moderate elbow commonly used in industries. The objective is to assess the extent of geometrical nonlinearity from each load. This was followed by internal pressure and in-plane moment loads acting simultaneously in a geometrically nonlinear analysis, to determine the coupling effect between the two loads.

RESULTS AND DISCUSSION

The stress which is used here is taken to be the effective stress factor (ESF), which is the ratio of the maximum von Mises effective stress to the nominal maximum stress given by simple theory for an equivalent straight pipe. For pressure loading, the nominal stress is the mean diameter hoop stress, $Pd_m/2t$, and for torsion and in-plane moment loading, the nominal stress is the maximum bending stress, Mr_o/I. The ESFs will be referred to as stress factors in the following text. The elbow models EL05 and EL07 were selected here for detailed discussion. The results of other elbows in the series were considered in the general discussion.

Effective hoop and axial stresses

The von Mises effective stress factor (ESF) is influenced by three geometrical factors - thickness, bend radius and pipe mean diameter, which can be grouped into two parameters, $b(=R/r_m)$ and d/t. The ESF distribution around the circumference at the elbow mid-section of elbows EL05 and EL07 are shown in Figures 1-3. Due to torsion (Figure 1), maximum stresses occur on the outer surface with peaks on either side of the crown, at θ=75° and 120°. The peaks are more pronounced in thinner elbows with d/t ≥80. At the intrados and extrados, the ESFs do not vary much with elbow thickness but elsewhere the stresses increase with thinner elbows, with stresses greater on the outer surface.

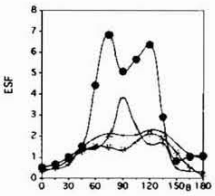

Figure 1

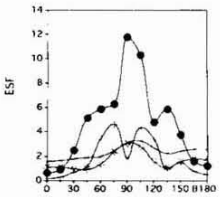

Figure 2

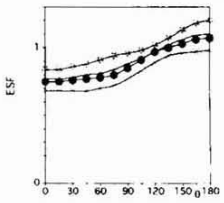

Figure 3

Key to markers X EL07-out ☆ EL07-in • EL05-out + EL05-in

Figures 1 — 3: von Mises stresses on outer and inner surfaces of model EL05 and EL07 - torsion, moment and pressure loading respectively

In Figure 2, an in-plane moment gives the same response as in torsion except that maximum stresses occur at θ=90°. However, in thicker elbows, there is a tendency for the stress magnitude on the outer surface at the intrados to approach that at the crown. Increasing the thickness and bend radius result in levelling of the peaks and reduction of stresses. For internal pressure (Figure 3), the stresses on both surfaces increase gradually from the extrados to the intrados, with stresses on the inner surface higher than on the outer surface but the stress gradient across the wall becomes smaller as the elbow gets thinner.

The pipe factor λ is defined as $\lambda=tR/r_m^2$ and the bend factor as $b=R/r_m$. Hence, $\lambda=(t/r_m)b$. If b is kept constant, the pipe factor λ is then inversely proportional to d/t ratio. On many occasions, in trying to show the effect of the bend ratio and pipe factor on stresses, analysts present the stress variation with λ and b. From Figures 4-6, for torsion and moment loads, stresses increase with decreasing λ, but there is no definite trend of stress variation with b. This is because λ is not an independent parameter which affects stress. If λ is kept constant, varying b results in a change of d/t too. This may explain the conflicting reports on the effect of λ on stress although the individual effect of d/t ratio and b is very clear.

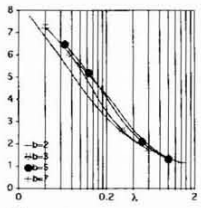

Figure 4

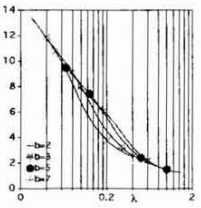

Figure 5

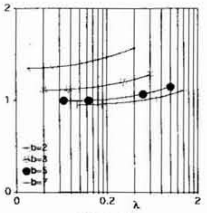

Figure 6

Figures 4 — 6: Influence of b and λ on maximum ESF - torsion, moment and pressure loading respectively

When the ESF results are presented as functions of d/t and b (Figures 7-9), a definite trend is observed, i.e. the ESFs increase with decreasing bend ratio b. For torsion and moment loads, when the pipe becomes thicker (low d/t), the ESFs become less affected by the pipe bend, as shown in Figures 7 and 8. It is also observed that in thin pipes (d/t>150), the maximum ESFs tend to be less affected by the d/t ratio. For pressure loading, the d/t ratio does not influence maximum ESFs but when the pipe becomes thicker (d/t<40), the ESFs increase with decreasing d/t (Figure 9). A tabular comparison of maximum ESFs due to the three load cases is shown in Table 2.

Table 2: Comparison of maximum von Mises ESF s

Model	Max.	Mises	ESF	Model	Max.	Mises	ESF
	Torsion	Moment	Pressure		Torsion	Moment	Pressure
EL01	7.74	13.39	1.35	EL09	6.48	9.5	1.0
EL02	6.33	10.8	1.36	EL10	5.19	7.44	1.0
EL03	3.17	3.8	1.47	EL11	2.10	2.44	1.07
EL04	2.17	2.56	1.57	EL12	1.32	1.53	1.15
EL05	7.25	11.79	1.11	EL13	5.65	7.99	0.95
EL06	6.05	9.33	1.12	EL14	4.45	6.24	0.96
EL07	2.61	3.25	1.20	EL15	1.74	1.93	1.03
EL08	1.74	2.14	1.28	EL16	1.16	1.30	1.11

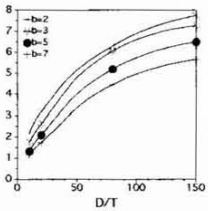

Figure 7

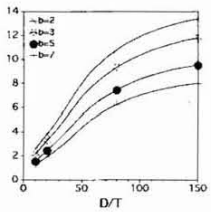

Figure 8

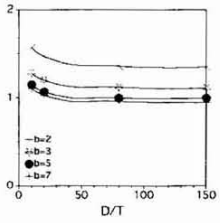

Figure 9

Figures 7 — 9: Influence of b and d/t on maximum ESF - torsion, moment and pressure loading respectively

Comparison with other analyses

The FEM hoop and axial stresses are compared to theoretical results which are computed from the energy method of Rodabaugh and George [4] and Subsection NB-3685 of ASME Section III [6] design code. For moment loading, the FEM results for the thicker model EL07 are in good agreement with theory but for the thinner EL05 model, the energy theory [4] can overpredict stresses by more than 100%. For torsion loading, the theoretical stresses are higher than the FEM, especially for the thinner model. For pressure, the stresses predicted by ASME are satisfactory. Thin elbows are likely to suffer from geometric nonlinear behaviour when subjected to moment and torsional loads, resulting in higher stresses than predicted by the present FEM linear analysis, which accounts for the large stress discrepancies. The agreement with model EL07 is satisfactory for moment and pressure loads but fair with torsional moment.

Some authors place great importance on the exact location of maximum stresses and how the stress peaks move along the pipe hoop direction as the geometric parameters vary. In this study, the stress peaks shift towards the crown as the elbow becomes thinner. With respect to this, the FEM shows good agreement with the findings of Fujimoto and Soh [13] and Sobel and Newman [21]. The position of the maximum hoop stress in the present study is also consistent with the finding of Findlay and Spence [11] who performed experimental tests on long radius elbows with in-plane moment. In another similar analysis, Thomson and Spence [16] noted that the maximum hoop stress occurs at $\theta=95^\circ$, and the stress was reported to increase with R/r_m ratio. The FEM shows that depending on λ, this location is either at $\theta=90^\circ$ or at $\theta=180^\circ$, but other authors specifically give the location as $\theta=90^\circ$. The ASME code implies the position to be at $\theta=90^\circ$.

The stress indices C_1 and C_2 in ASME [6] are essentially maximum elastic stress factors due to pressure and moment

loads respectively. Expressed in terms of elbow geometric parameters, the indices are defined as:-

$$C_1 = (2R\text{-}r_m) / 2(R\text{-}r_m)$$

$$C_2 = 1.95 / \lambda^{2/3}$$

The BS 806 [7] code presents the axial and hoop stress factors for in-plane and out-of-plane moments in graphical forms. For comparison, the hoop stress factors of the BS are selected as they are larger for the range of elbows under study. Table 3 compares the maximum ESF from the FEM with the stress indices from ASME and BS codes.

From Table 3, the ASME stress index for pressure C_1 does not differ much with the FEM results but for other loading, the ASME and BS results are quite similar in the way they differ from the FEM results at various values of d/t and b. The table shows an overall conservatism of both codes especially for torsion loading. The discrepancies become larger as the elbow becomes thinner and as the bend radii become smaller. From Fujimoto and Soh's [13] examination, they commented on ASME's overestimation of stress by about 40%. The Codes emphasise the increase of stress index as λ decreases because of progressive flattening of the cross-section. Furthermore ASME does not consider the effects of tangent pipes, resulting in overprediction of stresses, i.e. more conservative stresses.

Table 3: Maximum stress factor, at ϕ = 0ß - comparison between FEM, ASME [6] and BS [7]

		MAX. STRESS FACTOR						
METHOD	MODEL	TORSION	MOMENT	PRESSURE	MODEL	TORSION	MOMENT	PRESSURE
FEM	EL01	7.74	13.39	1.35	EL09	6.48	9.5	1.0
ASME		21.85	21.85	1.5		11.86	11.86	1.25
BS		19.5	23.0	-		10.7	11.5	-
FEM	EL02	6.33	10.8	1.36	EL10	5.19	7.44	1.0
ASME		14.37	14.37	1.5		7.8	7.8	1.25
BS		14.0	15.0	-		6.6	7.8	-
FEM	EL03	3.17	3.8	1.47	EL11	2.1	2.44	1.07
ASME		5.7	5.7	1.5		3.1	3.1	1.25
BS		6.2	6.2	-		2.9	3.0	-
FEM	EL04	2.17	2.56	1.57	EL12	1.32	1.53	1.15
ASME		3.59	3.59	1.5		1.95	1.95	1.25
BS		4.3	4.0	-		1.9	1.8	-
FEM	EL05	7.25	11.79	1.11	EL13	5.65	7.99	0.95
AME		16.67	16.67	1.25		9.48	9.48	1.08
BS		14.5	17.0	-		8.4	9.6	-
FEM	EL06	6.05	9.33	1.12	EL14	4.45	6.24	0.96
ASME		10.96	10.96	1.25		6.23	6.23	1.08
BS		10.0	11.5	-		5.4	6.0	-
FEM	EL07	2.61	3.25	1.20	EL15	1.74	1.93	1.03
ASME		4.35	4.35	1.25		2.47	2.47	1.08
BS		4.4	4.5	-		2.1	2.2	-
FEM	EL08	1.74	2.14	1.28	EL16	1.16	1.30	1.11
ASME		2.74	2.74	1.25		1.56	1.56	1.08
BS		2.9	2.9	-		1.3	1.2	-

Note

Maximum stress factor

For FEM, value refers to maximum Mises effective stress factor
For BS, value refers to maximum hoop or axial stress factor
For ASME, value refers to maximum hoop stress factor

Effect of attached pipes

The end conditions of the curved section affect elbows with small pipe factors. The tangent pipes resist ovalization of the cross-section so that stresses near the ends of the elbow are lower than at the mid-section where deformation is largest.

For pressure loading there is no ovalization and the stresses do not increase along the axial direction of the curved section. Due to torsion loading, for both elbow models EL05 and EL07, the maximum stresses at the mid curved section are about three times those at the bend ends. In-plane moment produces stress peaks which are about $1^1/_2$ times those at the bend ends. From the results of other elbow models, the bend radius rather than pipe thickness influences propagation of the end effects. For example, the ESFs of long radius elbow models EL13 and EL16 are reduced by about 50% at the elbow ends, while in models EL01 and EL04 the reduction is about 35%.

Geometrical nonlinearity and load coupling effect between pressure and moments (in-plane and torsional). Models EL01 and EL07.

The analysis of load coupling between internal pressure and moment is complex. It is well known that especially in thin elbows, an in-plane or torsional moment causes severe ovalization of the pipe cross-section. In a linear analysis, stresses from moment load are algebraically summed with those from pressure load. However, in reality the load interaction behaviour is more complex than superpositioning individual stresses because of the effect of load coupling. If the two loads act simultaneously, internal pressure stiffens the pipe such that ovalization is severely restricted when moment load acts. This results in a coupling between the two loads, and consequently in a reduction of flexibility and stresses.

Many researches have been devoted to the study of combined pressure and in-plane moment on elbows. Among the researchers are Rodabaugh and George [4] and Spence and Boyle [22] who studied the influence of pressure on stresses produced by moments. The results from the present study on the influence of pressure on this combined loading can be seen in Tables 4 and 5 where the combined stresses are derived from three methods. In the linear analysis, the combined stresses are obtained from linear elastic FEA of individual loads. In the second method, individual stresses which are obtained from geometrically nonlinear FEA are again combined algebraically. In the third method the loads act simultaneously in a geometrically nonlinear FEA. The last method shows the effect of load coupling, if any.

Table 4: Effective stresses from linear and nonlinear FEM analyses - elbow model EL01

Loading	Geometric nonlinear	Geometric nonlinear and simultaneous loading
	Max. σ_{vM} % difference from linear analysis	Max. σ_{vM} % difference from linear analysis
P	0	-
M	9.1	-
-M	-13.3	-
P+M[a]	8.3	- 33.2
P+(-M)[b]	-11.5	- 50.9

All the stresses in the above table occur at the crown.

Table 5: Effective stresses from linear and nonlinear FEM analyses - elbow model EL07

Loading	Geometric nonlinear	Geometric nonlinear and simultaneous loading
	Max. σ_{vM}% difference from linear analysis	Max. σ_{vM}% difference from linear analysis
P	0	-
	0	
M	5.6	-
-M	-4.4	-
P+M[a]	5.0	- 3.4
P+(-M)[b]	-3.9	- 9.3

a pressure + closing in-plane moment

b pressure + opening in-plane moment

The third method evidently shows the stiffening effect of internal pressure on in-plane moment, especially on the thinner model EL01. With the specified combination of pressure and opening moment, the stress is reduced by about 51%, and with a closing moment the reduction is about 33%. The thicker model EL07 shows smaller corresponding reductions of 9.3 and 3.4%.

From geometric nonlinear analysis, an in-plane closing moment causes stresses at the crown to increase progressively with load but an in-plane opening moment causes a progressive reduction of the stress increase. Although small, the nonlinear effect in model EL01 is twice that of EL07. Pressure loading showed no signs of geometric nonlinear effect.

The effect of geometric nonlinearity on stiffening of the cross-section shows interesting results. A closing moment increases the maximum effective stress, and an opening moment reduces the stress. These increment and reduction are larger in the thinner model EL01. When the results from both geometric nonlinearity and load coupling analyses are examined closely, the trend becomes apparent. In geometric nonlinear analysis, the increase is due to the tensile stresses from the closing moment being added to the tensile pressure stresses at the outer surface of the crown. An opening moment load produces compressive stresses at the same location, hence providing a reducing effect to the pressure stresses. When the load coupling effect is taken into account, the stiffening effect from internal pressure reduces ovalization and has a cancelling effect on the stress produced by geometric deformation. This effect of load coupling is large in the thinner elbow model.

In the final load coupling analysis, the moment-pressure load interaction results in lower maximum stresses than produced by individual loads, hence the yield envelopes of load interaction curves are larger. A detailed study of load interaction is given in Ref. [23]. Elbows with higher yield limits have larger yield envelopes because the stresses become progressively reduced as the moment is increased.

The moment-pressure interaction of the thicker model EL07 does not exhibit much load coupling effect, unlike the thinner model EL01. Geometric nonlinear analysis gives slightly lower maximum stresses than linear analysis. This results in the linear analysis of first yield envelope to be slightly more conservative than the nonlinear envelope.

In moment-pressure interaction, both nonlinear and load coupling effects show an increase in the first yield opening moment carrying capacity of the elbows. The yield locus indicates that for the thicker elbow, there is a slight increase in the (opening) moment carrying capacity at low internal pressures. There is also an increase in internal pressure carrying capacity at low values of opening moment, which are not shown by the thinner elbow nor for closing moments.

The phenomena of geometric nonlinearity and load coupling effect are similarly encountered in pressure-torsion interaction, i.e. the reduction of maximum stress is due to both phenomena. In the thinner model EL01, the torsion load shows large nonlinear and load coupling effects. The nonlinear yield envelope of the thinner model is found to be very conservative compared to the thicker model. In model EL01 since the effects of geometric and load coupling become increasingly large at high yield stress, the torsion-carrying capacity of the elbow increases with stress limit. At all yield limits, the torsion is increased beyond T_Y when $P \leq 0.5P_Y$.

Load interaction from Codes

BS 806

In BS 806 [7] the hoop, axial and shear stresses are based on thin pipe theory. Moreover, the effects of pressure and moment are not coupled, thus making the interaction procedure conservative. The symbols used are in accordance with the respective codes.

Torsion-Pressure interaction

The total hoop stress f_T is the sum of separate effects from internal pressure and torsion loading and is given by:-

$$f_T = pd/2t + 0.5p + 0$$

and similarly, the total axial stress is:-

$$f_L = pd^2/4t(d + t) + 0$$

Since there is no contribution of shear stress from pressure, the total shear stress is:-

$$f_s = M_T(d + 2t)/4I$$

and since $f_T > f_L$, the effective stress is:-

$$f_e = \sqrt{(f_T^2 + 4f_s^2)} = Y$$

or

$$(pd/2t + 0.5p)^2 + 4[M_T(d + 2t)/4I]^2 = Y^2$$

to give a circular interaction $\quad \bar{T}^2 + \bar{P}^2 = 1$

Moment-Pressure interaction

Similarly, when internal pressure and in-plane moment act together,

Total $\quad f_T = pd/2t + 0.5p + rM_iF_{Ti}/I$

Total $\quad f_L = pd^2/4t(d + t) + rM_iF_{Li}/I$

For a given value of pipe factor, $F_{Ti} > F_{Li}$ so that $f_T > f_L$. Since M_T is not acting, the shear stress $f_s = 0$. Substituting for the value of f_T into the equation for f_e,

$$(pd/2t + 0.5p + rM_iF_{Ti}/I)^2 + 0 = Y^2$$

which gives a linear relation $\quad \bar{M} + \bar{P} = 1$

Moment-Torsion interaction

Similar to the previous section,

Total $\quad f_T = 0 + rM_iF_{Ti}/I$

Total $\quad f_L = 0 + rM_iF_{Li}/I$

As before $f_T > f_L$, hence giving $F = f_T$.

From torsion loading, $\quad f_s = M_T(d + 2t)/4I$

The effective stress, $\quad f_e = \sqrt{(F^2 + 4f_s^2)} = Y$

or $\quad (rM_iF_{Ti}/I)^2 + 4[M_T(d + 2t)/4I]^2 = Y^2$

to give a circular relation $\quad \bar{M}^2 + \bar{T}^2 = 1$

ASME III

Equation (10) of Subsection NB-3653.1 ASME III [6] code is meant to control primary plus secondary loads so as to place an upper bound on deformations. Neglecting thermal effects, Equation (10) of ASME is given by:-

$$C_1P_0D_0/2t + C_2D_0M_i/2I \leq 3S_m$$

where the resultant moment $\quad M_i = \sqrt{(M_x^2 + M_y^2 + M_z^2)}$

The above equations result in a circular moment-torsion interaction,

$$\bar{M}^2 + \bar{T}^2 = 1$$

and linear torsion-pressure and moment-pressure interactions,

$$\bar{T} + \bar{P} = 1$$

and $\quad \bar{M} + \bar{T} = 1$

In the Codes the maximum hoop stresses due to the individual loads are summed, regardless of their location on the pipe. In the present method, stresses at every nodal point are determined for every load combination and subsequently the maximum stress is located. Hence in this method the maximum stress may not be at the locations of maximum stress due to individual loads.

First yield load interaction — comparison between FEM, BS and ASME

The load interaction results from FEM [23] are listed in Table 6. The moment-torsion and torsion-pressure interactions are clearly best represented by circular and linear interactions respectively. Taking into consideration the behaviour of a wide range of elbows, the most appropriate moment-pressure interaction is linear. The results from BS and ASME are listed for comparison. In the ASME code, the interactions are similar to the FEM but in the BS code, only the circular torsion-pressure interaction is different from the FEM.

Table 6: First yield load interaction — comparison between FEM, BS and ASME

	FEM	BS	ASME
Moment-Torsion			
Exact relation		$(rM_iF_{Ti}/I)^2+4[M_T(d+2t)/4I]^2=Y^2$	
Equivalent relation	$\bar{M}^2 + \bar{T}^2 = 1$	$\bar{M}^2 + \bar{T}^2 = 1$	$\bar{M}^2 + \bar{T}^2 = 1$
Torsion-Pressure			
Exact relation		$(pd/2t+0.5p)^2+4[M_T(d+2t)/4I]^2=Y^2$	
Equivalent relation	$\bar{T} + \bar{P} = 1$	$\bar{T}^2 + \bar{P}^2 = 1$	$\bar{T} + \bar{P} = 1$
Moment-Pressure			
Exact relation		$(pd/2t+0.5p+rM_iF_{Ti}/I)^2=Y^2$	
Equivalent relation	$\bar{M} + \bar{P} = 1$	$\bar{M} + \bar{P} = 1$	$\bar{M} + \bar{P} = 1$

CONCLUSIONS

The major conclusions to be drawn from this work are:-

1. For moment and torsion loading, the maximum ESF increases as d/t increases or as b decreases. As the elbow becomes thicker, the maximum ESF is less affected by b. For internal pressure, when d/t >40 and b>5, the maximum ESF is not affected by parameters d/t and b.
2. The ASME result for torsion loading is suspect. For moment loading, they are more conservative for low values of λ. Although slightly less conservative, the BS 806 code is satisfactory in determining the maximum ESF for moment load.
3. The moment-torsion and torsion-pressure first yield load interactions are not significantly affected by R/r_m and d/t ratios. The moment-pressure interaction is not much affected by R/r_m but significantly affected by d/t.
4. In certain cases, a combined loading of internal pressure and in-plane moment causes a reduction in maximum ESF which can be quite considerable in thin elbows (d/t>80).
5. Compared to the FEM, the BS rules are conservative for torsion-pressure interaction. The ASME load interaction agrees with the FEM.
6. From the FEM, it is proposed that the torsion-pressure and moment-pressure interactions be taken to be linear and the moment-torsion interaction to be circular. For the moment-pressure interaction, if the linear relation is assumed, for elbows of specific geometries, the effective stresses can be significantly conservative.
7. The increase in in-plane moment or torsion carrying capacity is mainly due to load coupling effect, with thinner elbows being largely affected.
8. In both moment-pressure and torsion-pressure load interactions, the maximum moment or torsion carrying capacity is not necessarily achieved at high internal pressures. From the thinner elbow model EL01, the maximum von Mises stresses are greatly reduced between $P=0.2P_Y$ and $P=0.5P_Y$.
9. For the thick elbow model, the results from linear analysis gives a satisfactory correlation with an analysis which includes geometric nonlinearity and coupling effect. Since all the linear load interaction curves are more conservative, the plots which are produced for elbows with about the same geometric parameters as EL07, can be used to predict first yield behaviour with high accuracy.

REFERENCES

[1] T. von Karman, Uber die Formanderung dunnwandinger Rohre, insbesondere federnder Ausgeichrohre , Zeit VDI, Vol. 55, pp. 1889-1895, 1911.

[2] I. Vigness, Elastic Properties of Curved Tubes , Trans. ASME, Vol. 65, pp. 105-120, 1943.

[3] P.G. Kafka and M.B. Dunn, Stiffness of Curved Circular Tubes with Internal Pressure , Trans. ASME Journal Applied Mechanics, Vol. 78, pp. 247. 1956.

[4] E.C. Rodabaugh and H.H. George, Effect of Internal Pressure on Flexibility and Stress Intensification Factors of Curved Pipe or Welding Elbows , Trans. ASME, Vol. 79, pp. 939-948, 1957.

[5] N. Gross, Experiments on Short-Radius Pipe Bends , Proc. Int. Mech. Eng., pp. 465-479, 1952-1953.

[6] ASME Boiler and Pressure Vessel Code, Div. I, Section III, Nuclear Power Plant Components. 1981.

[7] BS 806:1986 - Design and Construction of Ferrous Piping Installations for and in Connection with Land Boilers.

[8] C.E. Turner and H. Ford, Examination of the Theories for Calculating the Stresses in Pipe Bends Subjected to In-plane Bending , Proc. Instn. Mech. Engrs., Vol. 171, pp. 513-525, 1957.

[9] R.T. Smith, Theoretical Analysis of the Stresses in Pipe Bends Subjected to Out-of-plane Bending , Journal of Mech. Eng. Science, Vol. 9, pp. 115-123, 1967.

[10] T.E. Pardue and I. Vigness, Properties of Thin Walled Curved Tubes of Short Bend Radius , Trans. ASME, Vol. 73, pp. 77-84, 1951.

[11] G.E. Findlay and J. Spence, Stress Analysis of Smooth Curved Tubes with Flanged End Constraints , Int. Journal of Pressure Vessel & Piping, Vol. 7, pp. 83-103, 1979.

[12] H.A. Lang, Mean Stresses and Mean Displacements in Thin-Walled Curved Circular Tubing , Int. Journal Pressure Vessel & Piping, Vol. 21, pp. 67-78, 1985.

[13] T. Fujimoto and T. Soh, Flexibility Factors and Stress Indices for Piping Components with D/T‡100 Subjected to In-plane or Out-of-plane Moment , Trans. of ASME, Vol. 110, pp. 374-386, 1988.

[14] W.G. Dodge and S.E. Moore, Stress Indices and Flexibility Factors for Moment Loadings on Elbows and Curved Pipe , WRC, Vol. 179, pp. 1-19, 1972.

[15] H. Ohtsubo and O. Watanabe, Stress Analysis of Pipe Bends by Ring Elements , ASME Journal Pressure Vessel Tech., Vol. 100, pp. 112-122, 1978.

[16] G. Thomson and J. Spence, Maximum Stresses and Flexibility Factors of Smooth Pipe Bends with Tangent Pipe Terminations under In-plane Bending , Journal of Pressure Vessel Technology, Vol. 105, pp. 329-336, 1983.

[17] R. Natarajan and J.A. Blomfield, Stress Analysis of Curved Pipes with End Restraints , Computers and Structures, Vol. 5, pp. 187-196, 1975.

[18] A.B. Ayob, Load Interaction in Pressurised Structures Using The Finite Element Method , Int. Conf. on Pipes and Pressure Vessels, Singapore, 1996.

[19] PATRAN-G. Release 2.5. PDA Engineering. 1990 Edition.

[20] ASAS-H Finite Element System. WS Atkins Engineering Science. 1989 Edition.

[21] L.H. Sobel and S.Z. Newman, Comparison of Experimental and Simplified Analytical Results for In-Plane Plastic Bending and Buckling of an Elbow , Jour. Pres. Ves. Tech., Vol.102, pp. 400-409, 1980.

[22] J. Spence and J.T.A. Boyle, A Simple Analysis for Oval, Pressurised Pipe Bends under External Bending , 4th Int. Conf. Pres. Ves. Tech. London, 1980.

[23] A.B. Ayob, The Interaction of Pressure, In-Plane Moment, and Torque Loadings on Piping Elbows , submitted for publication, 2003.